Electronic Supplementary Material (ESI) for Journal of Materials Chemistry A.

Supporting Information

Morphology Controllable Synthesis of PtNi Concave Nanocubes Enclosed by High-Index Facets Supported on Porous Graphene for Enhanced Hydrogen Evolution Reaction

Juntao Yang, Guoqing Ning, Lei Yu, Yao Wang, Chenglong Luan, Aixin Fan, Xin Zhang,* Yujie Liu, Yin Dong, Xiaoping Dai

State Key Laboratory of Heavy Oil Processing, China University of Petroleum, Beijing 102249, P. R. China. E-mail: zhangxin@cup.edu.cn

Experimental Section

Chemicals and reagents: MgO powder was purchased from Sinopharm Chemical Reagent Co. Ltd. Hexachloroplatinic acid with six water ($H_2PtCl_6 \cdot 6H_2O$) and Nickel chloride with six water ($NiCl_2 \cdot 6H_2O$) were analysis reagent (A. R.) and purchased from Sinopharm Chemical Reagent Co. Ltd. Poly(vinylpyrrolidone) (PVP, MW=30000) and glycine were A. R. and purchased from Sinopharm Chemical Reagent Co. Ltd. Commercial Pt/C (20 wt%) and Nafion were purchased from Alfa Aesar. Commercial porous carbon Vulcan XC-72 was purchased from Cabot Corporation. Sulfuric acid was A. R. and purchased from Sinopharm Chemical Reagent Co. Ltd. Graphene was prepared by the exfoliation of expanded graphite using shear-assisted super critical carbon dioxide. All reagents were used as received without further purification. Deionized (DI) water was used in all the experiments.

Preparation of catalysts:

Synthesis of porous graphene (PG):

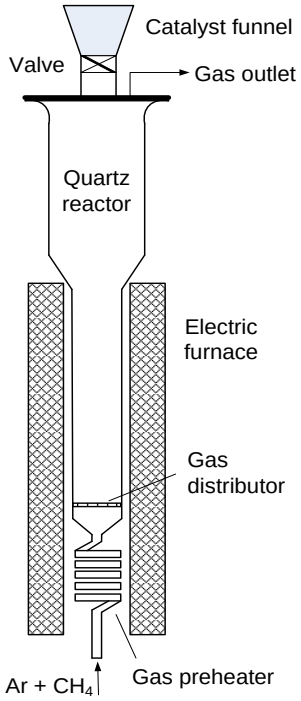

Fig. S1 Schematic of the downer reactor for the synthesis of the porous graphene.

Porous graphene used in this paper was synthesized by a chemical vapor deposition (CVD) process using porous MgO layers as templates.[1] First, MgO power was mixed with deionized water accompanied with ultrasonic agitation. The mixture was boiled for 24 h in a reflux apparatus. After filtration and drying, the material obtained was ground into a fine powder. The powder was calcined at 500 ℃ for 30 min to remove

water. Porous graphene was synthesized by CH_4 cracking at 875 ℃ in a vertical quartz reactor with diameter of 50 mm and length of 1500 mm. A sintered porous plate was used as the gas distributor at the bottom of the reactor. Gas entered the bottom preheater of the reactor, then passed through the gas distributor, and finally flowed out into the atmosphere. On the top of the quartz reactor, there was a stainless steel plate with a hopper for feeding catalyst. In a typical run, the quartz reactor was mounted in an electrical tube furnace and was heated to 875 ℃ in an argon flow of 1000 ml/min at atmosphere pressure. Once the reaction temperature was reached, 500 mL/min CH_4 was introduced into the reactor. Then, the MgO template (about 30 g) was fed into the reactor over 5 min from the top hopper. After 10 min carbon deposition, CH_4 was turned off and the reactor was cooled to room temperature in an Ar atmosphere. The as-obtained material was collected for purification.

Synthesis of PtNi concave nanocubes (CNCs): In a typical synthesis, PVP (220 mg, MW=30000) glycine (38 mg), aqueous $NiCl_2$ solution (4 mL, 1.66 mM) and aqueous H_2PtCl_6 solution (1 mL, 20 mM) were mixed and stirred for 30 min, then sonicated in an ultrasonic bath for 5 min at room temperature. The resulting homogeneous yellow solution was transferred to a 20 mL Teflon-lined stainless-stell autoclave. The sealed vessel was heated at 200 ℃ for 6 hours before it was cooled to room temperature. The products were separated by centrifugation at 9900 rpm for 15 min and further purified by washing with aqueous ethanol solution three times.

PVP-Functional PG: m mg (m=5, 10, 20) PG, 2 mL deionized water and 220 mg PVP were mixed and stirred for 12 h and formed suspensions with different PG concentration.

Synthesis of PtNi/mPG CNCs: Glycine (38 mg), aqueous $NiCl_2$ solution (4 mL, 1.66 mM) and aqueous H_2PtCl_6 solution (1 mL, 20 mM) were added into PVP-functional PG suspensions mentioned above and stirred for 30 min, then sonicated in an ultrasonic bath for 5 min at room temperature. The resulting solutions were transferred to a 20 mL Teflon-lined stainless-steel autoclave. The sealed vessels were heated at 200 ℃ for 9 h before it was cooled to room temperature. The products were separated by centrifugation at 9900 rpm for 15 min and further purified by washing with aqueous ethanol solution three times.

PVP-Functional graphene (G) and PVP-Functional Vulcan XC-72 (C): 10 mg graphene or 10 mg Vulcan XC-72, 2 mL deionized water and 220 mg PVP were mixed and stirred for 12 h and formed suspension.

Synthesis of PtNi/10G CNCs and PtNi/10C CNCs: The synthesis method was the

same as that of PtNi/mPG CNCs, except that PVP-functional PG was replaced by PVP-functional G and PVP-functional C.

Synthesis of PtNi CNCs/10PG: After the synthesis and purification of PtNi CNCs, 2 mL deionized water and 10 mg PG were added and stirred for 12 h. The final product was collected then.

Characterization: The morphology and structure were observed by field-emission sacanning electron microscopy (FESEM, FEI, Quanta 200F). The size and morphology of the samples were determined by JEM 2100 transmission electron microscope (TEM) at 200 kV, and a Tecnai G2 F20 S-Twin high-resolution transmission electron microscope (HRTEM) operating at 200 kV. The samples were prepared by dropping ethanol dispersion onto carbon-coated copper grids with a pitettor, and the solvent was allowed to evaporate for TEM detection. The high-angle annular dark-field scanning TEM (HAADF-STEM) was determined by Tecnai G2 F20 S-Twin high-resolution transmission electron microscope (HRTEM) operating at 200 KV. The X-ray diffraction (XRD) patterns of samples were recorded on a Bruker D8-advance X-ray powder diffractometer operated at voltage of 40 kV and current of 40 mA with CuK radiation (λ = 1.5406 Å). Raman spectrometer (Renishaw RM2000) with the 532 nm wavelength. X-ray photoelectron spectrum (XPS) analysis was performed on a PHI 5000 Versaprobe system using monochromatic Al Ka radiation (1486.6 eV). All binding energies were referenced to the C 1s peak at 284.6 eV. And the Pt and Ni contents of each catalysts were measured by using inductively coupled plasma – optical emission spectrometry (ICP-OES). N_2 adsorption/desorption isotherms were determined by the Brunauer-Emmett-Teller (BET) method on Micomeritics JW-BK222 at liquid-nitrogen temperature. The pore size distribution was obtained from the desorption branch of the Barrett-Joyner-Halenda (BJH) method.

Electrochemical measurements: Electrochemical experiments were carried out using CHI 760e electrochemical analyzer (CHI Instrument, CHN). A conventional three-electrode cell was used, including a saturated calomel electrode (SCE) as reference electrode, a carbon plate as the counter electrode, and a glassy carbon electrode (3 mm in diameter) as the working electrode. A GC electrode was carefully polished with Al_2O_3 paste, and washed with deionized water before each experiment. After the electrode was dried, 3 μL suspension of well dispersed catalyst in a mixture of water and ethanol (2 mg mL^{-1}) was dropped onto the GC electrode. Before each electrochemical test, the electrode was illuminated by UV lamp (10 W, with 185 and 254 nm emissions) for 12 h to remove the capping agents.[2] The electrode then

covered with 3μL of 0.05 wt% Nafion (Alfa Aesar) and dried under the infrared lamp for 5 min. HER tests were conducted in a N_2 saturated aqueous solution of 0.5 M H_2SO_4 at room temperature. The potential range was from 0.045 to -0.155 V (vs. RHE) and the scan rate was 10 mV/s. Before measurements, the samples were pretreated by performing the cyclic voltammetry (CV) for 50 cycles from 0.005 to 1.245 V (vs. RHE) at a scan rate of 50 mV/s in the electrolyte. All polarization curves were iR-corrected. Electrochemical impedance spectroscopy measurements were investigated in the frequency range from 100 kHz to 0.01 Hz with AC amplitude of 35 mV under N_2-saturated solution.

Calculation of ECSA[3] and HER activities: To obtain ECSA value, CV was performed by cycling between 0.005 and 1.245 V (vs. RHE) at a scan rate of 50 mV/s in the electrolyte after purging with N_2. The last CV curve was applied to determine the hydrogen desorption charge (Q_H) derived from the following equation S1:

$$Q_H\,(C) = \int_{0.005}^{0.4} \frac{j \times dE}{v} \quad (S1)$$

Where the units of Q_H, j (current), E (potential), and v (scan rate) are C, A, V and V/s. The ECSA value was then calculated according to the equation S2:

$$ECSA = \frac{Q_H}{m \times q_H} \quad (S2)$$

Where m is the weight of Pt (g), q_H is the charge required for monolayer adsorption of hydrogen on a Pt surface, and the theoretical value of q_H is 210 μC cm^{-2}.

To derive the specific and mass HER activities, the LSV curve was measured in N_2-satuated H_2SO_4 solution (0.5 M) at a scan rate of 10 mV s^{-1}. Based on the ECSA, the specific activity was calculated according to the equation S3:

$$J = \frac{j \times q_H}{Q_H} \quad (S3)$$

With the basis of weight of Pt, the mass activity was calculated from the equation S4:

$$J' = \frac{j}{m} \quad (S4)$$

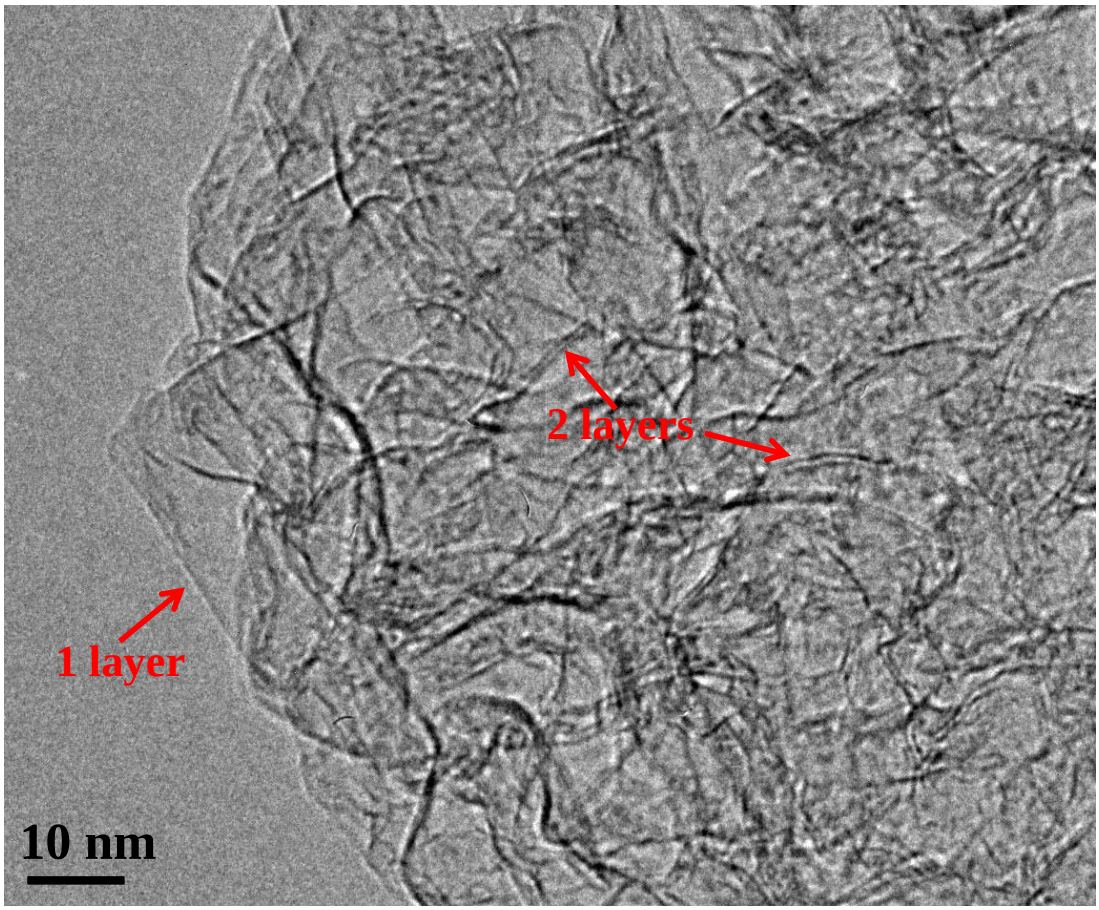

Fig. S2 HRTEM image of PG.

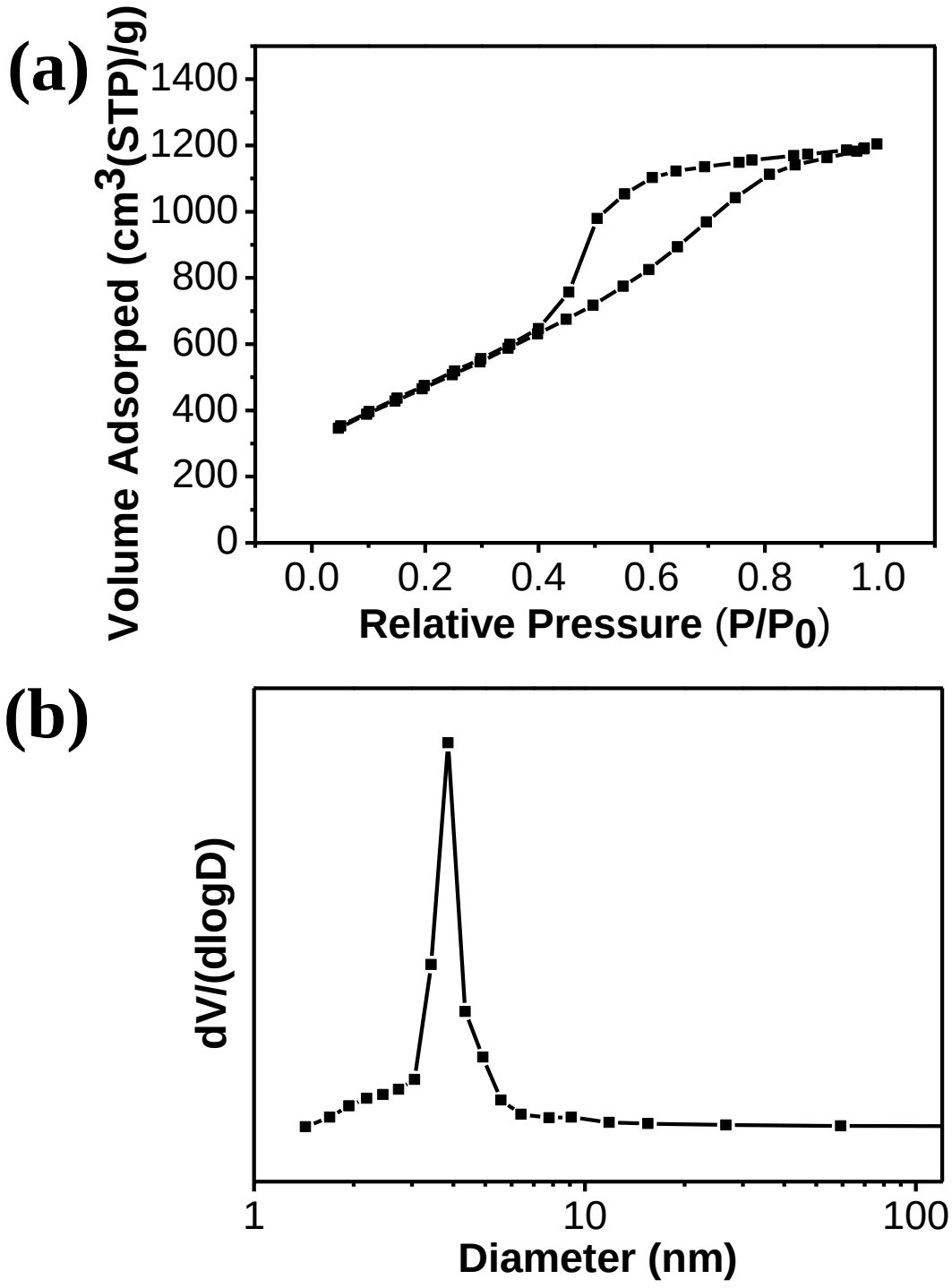

Fig. S3 (a) N_2 adsorption/desorption isotherms and (b) pore size distribution of PG.

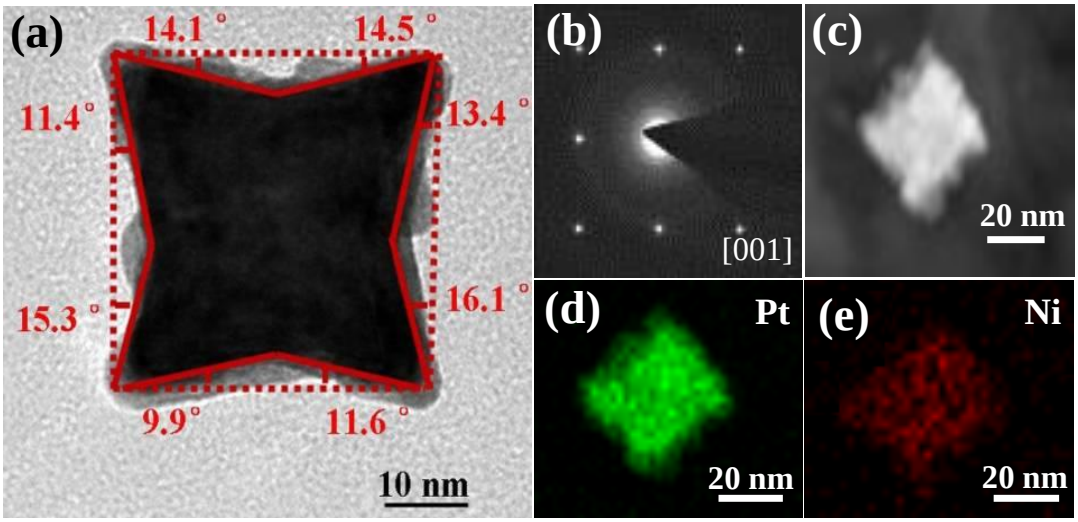

Fig. S4 (a) HRTEM, (b) corresponding SAED pattern, (c) HAADF-STEM image and (d and e) EDS mapping images of PtNi CNCs.

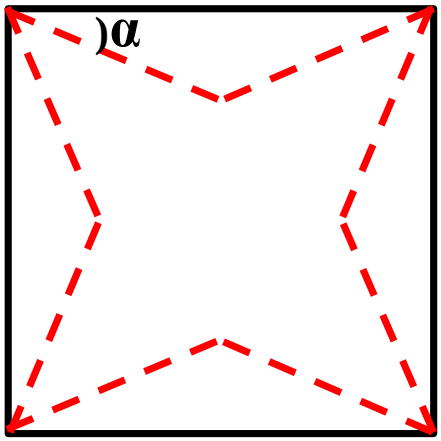

{hk0}	α (°)
{810}	7.1
{710}	8.1
{610}	9.5
{510}	11.3
{410}	14.0
{720}	15.9
{310}	18.4
{830}	20.6

Fig. S5 The theoretical relationship between interfacial angles and facets for HIFs.

A Miller index was used to describe crystal plane. The angle θ between two crystals $(h_1k_1l_1)$ and (h_2kl_2) is

$$\theta = \arccos\left(\frac{h_1h_2 + k_1k_2 + l_1l_2}{\sqrt{(h_1^2 + k_1^2 + l_1^2)(h_2^2 + k_2^2 + l_2^2)}}\right).$$

When the Z-axis intercept is infinite, the crystal planes are written (hk0). The angle between (hk0) and (100) can be calculated by

$$\alpha = \arccos\left(\frac{h}{\sqrt{h^2 + k^2}}\right).$$

The integers are usually written in lowest terms, we can get h and k from angle α.

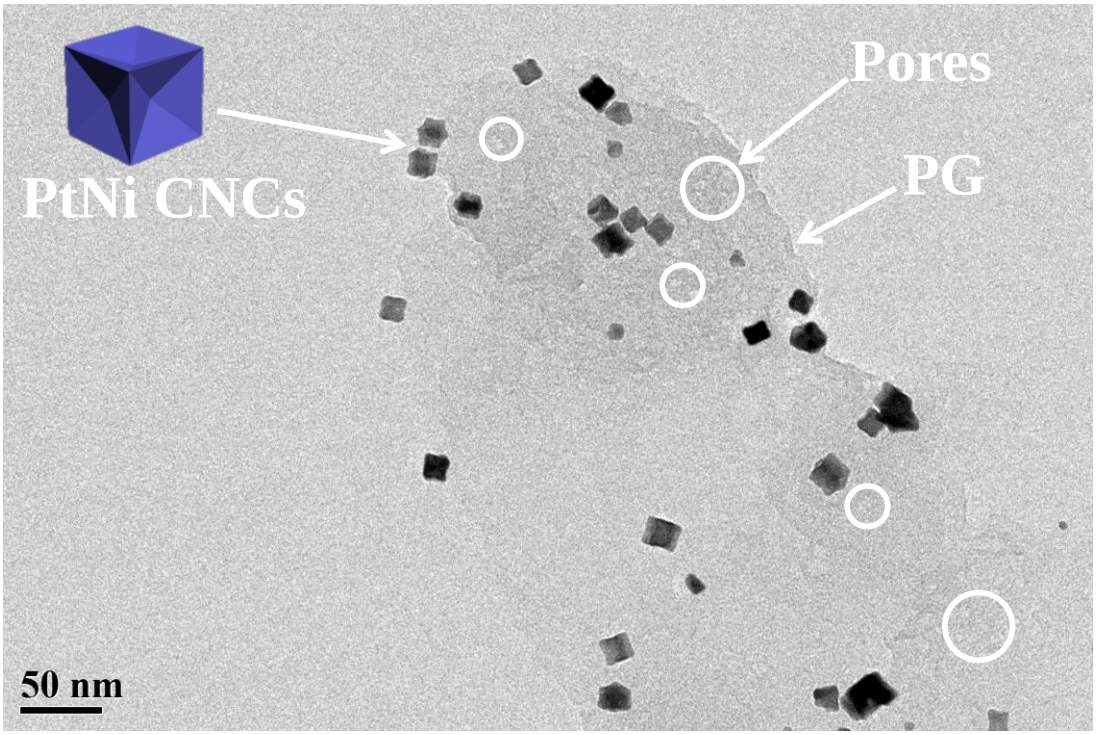

Fig. S6 TEM image of PtNi/10PG CNCs.

Table S1 Angle and size comparison of different CNCs.

Catalysts	Maximum angle (°)	Minimum angle (°)	Average angle (°)	Average size (nm)
PtNi CNCs	16.1	9.9	13.3	57.2
PtNi/5PG CNCs	12.3	7.8	9.6	41.1
PtNi/10PG CNCs	11.7	7.4	9.5	32.2
PtNi/20PG CNCs	9.2	4.1	7.1	12.5

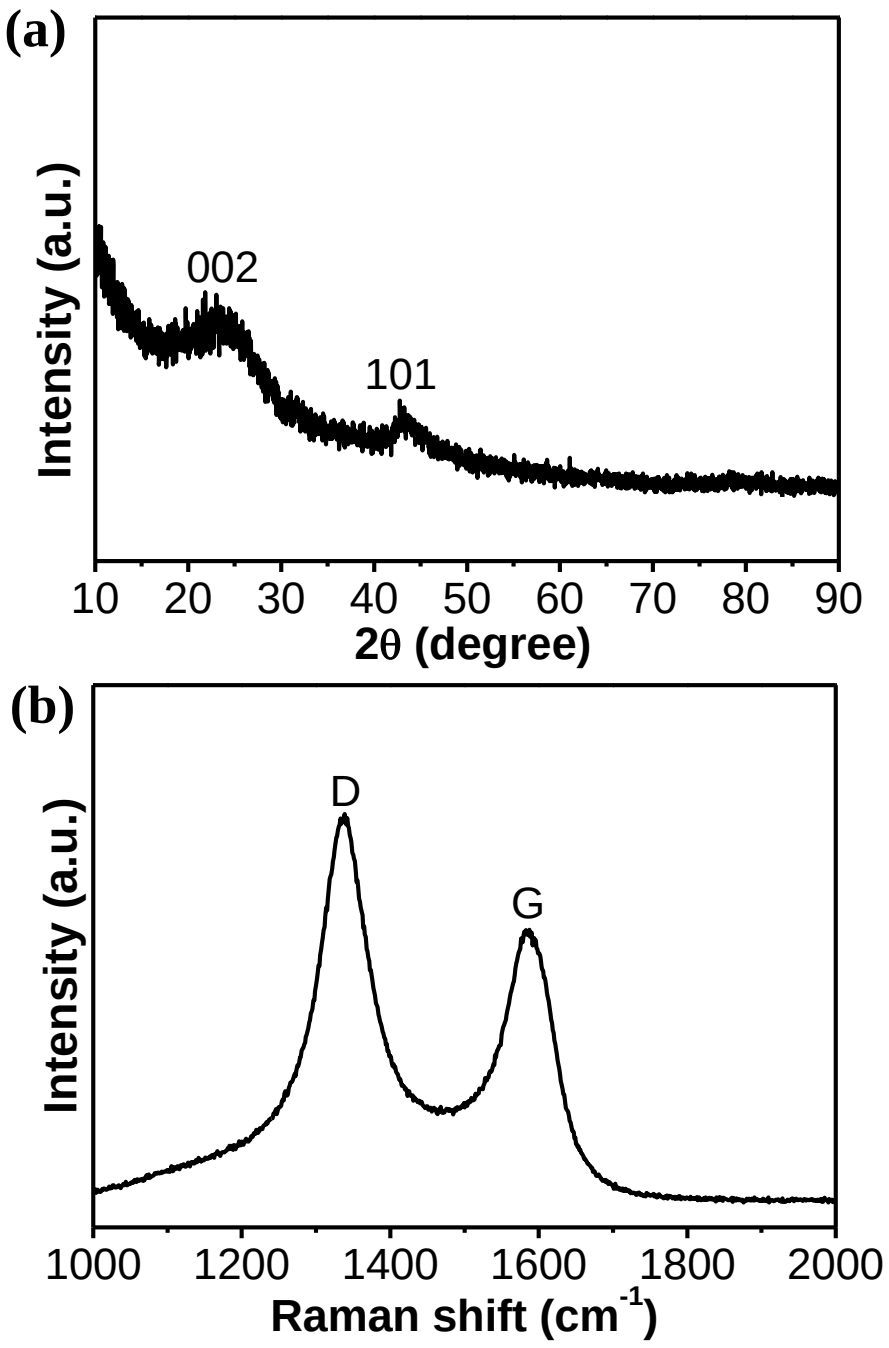

Fig. S7 (a) XRD pattern (b) Raman spectrum of the PG.

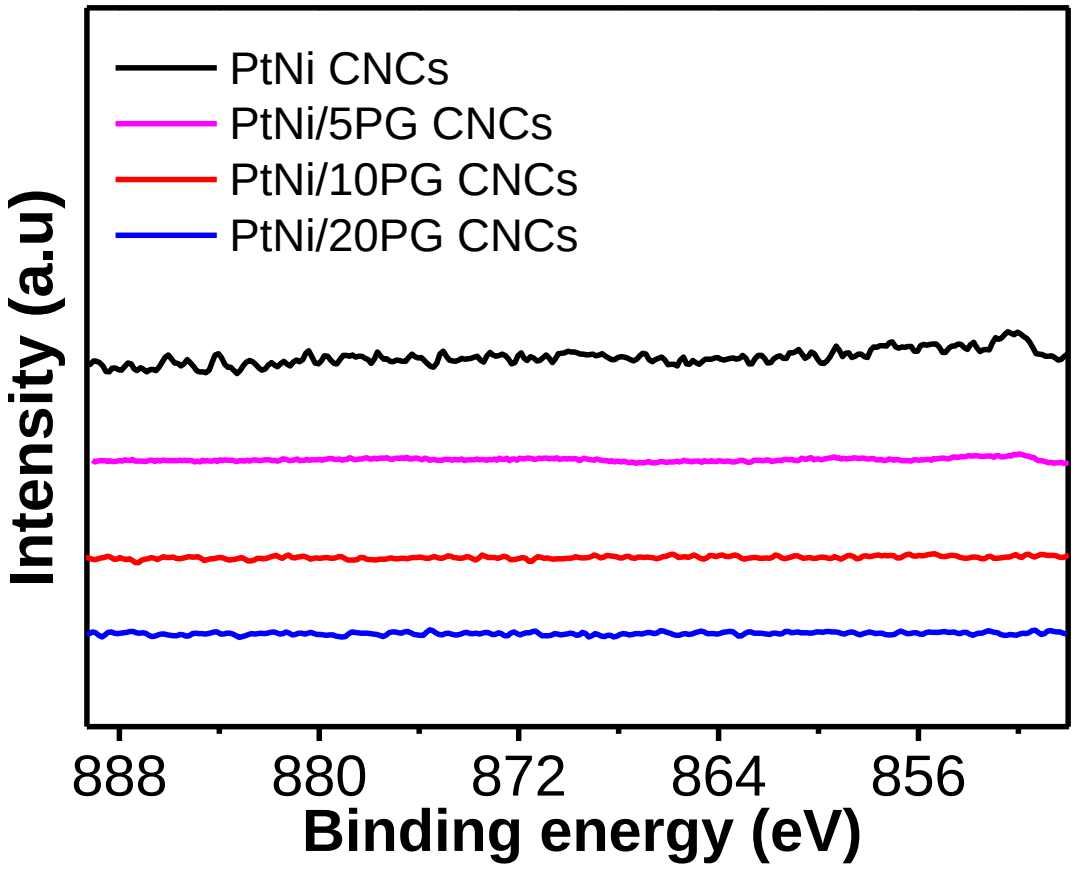

Fig. S8 Ni 2p XPS spectra of PtNi CNCs, and PtNi/mPG CNCs.

Table S2 Mass percentage of as-prepared catalysts measured by ICP-OES.

Catalysts	Total sample weight (T), [a] mg	Pt weight, [b] mg	Pt/T, %	Pt : Ni, mass ratio
PtNi CNCs	0.66	0.62	94.40	16:1
PtNi/5PG CNCs	4.97	0.99	19.93	13:1
PtNi/10PG CNCs	12.7	1.15	9.06	11:1
PtNi/20PG CNCs	24.93	0.92	3.69	7:1

[a] The total samples weight is used to measure the Pt and Ni weight during the ICP-OES analysis;

[b] The actual Pt weight is determined for the corresponding the total sample weight.

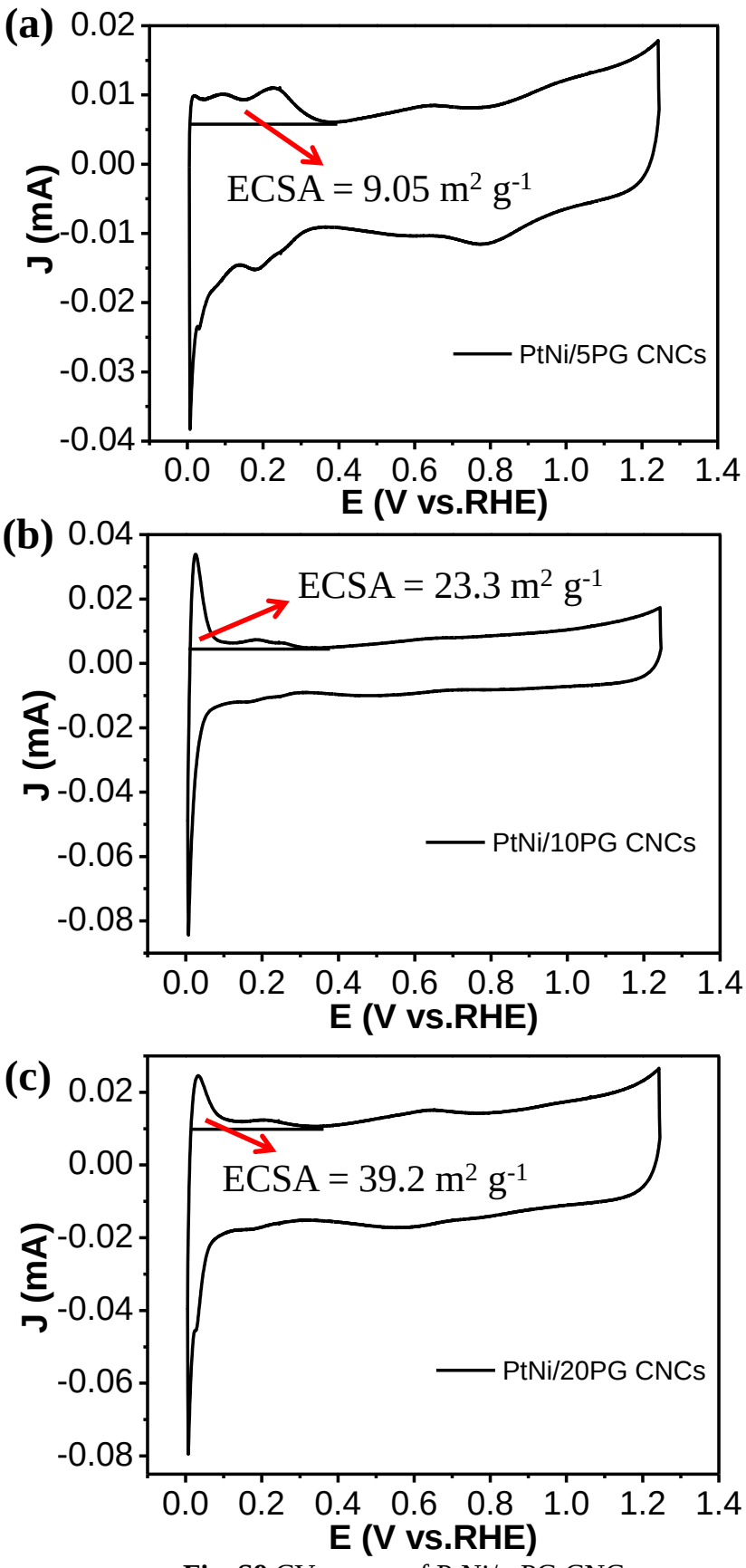

Fig. S9 CV curves of PtNi/mPG CNCs.

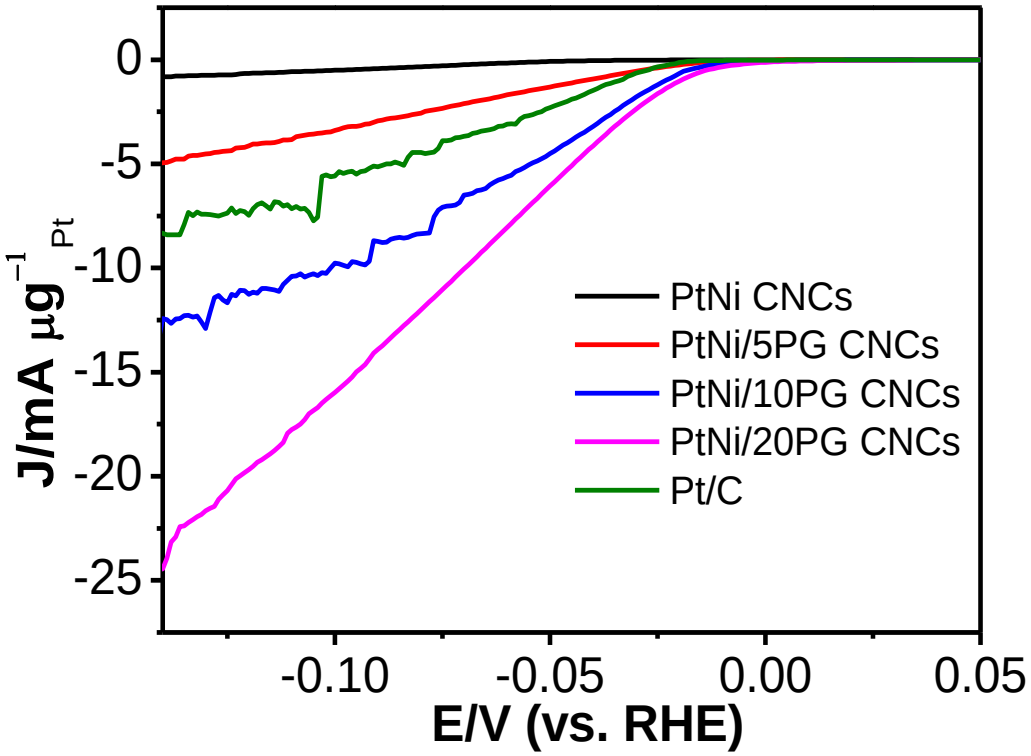

Fig. S10 Mass activity for HER.

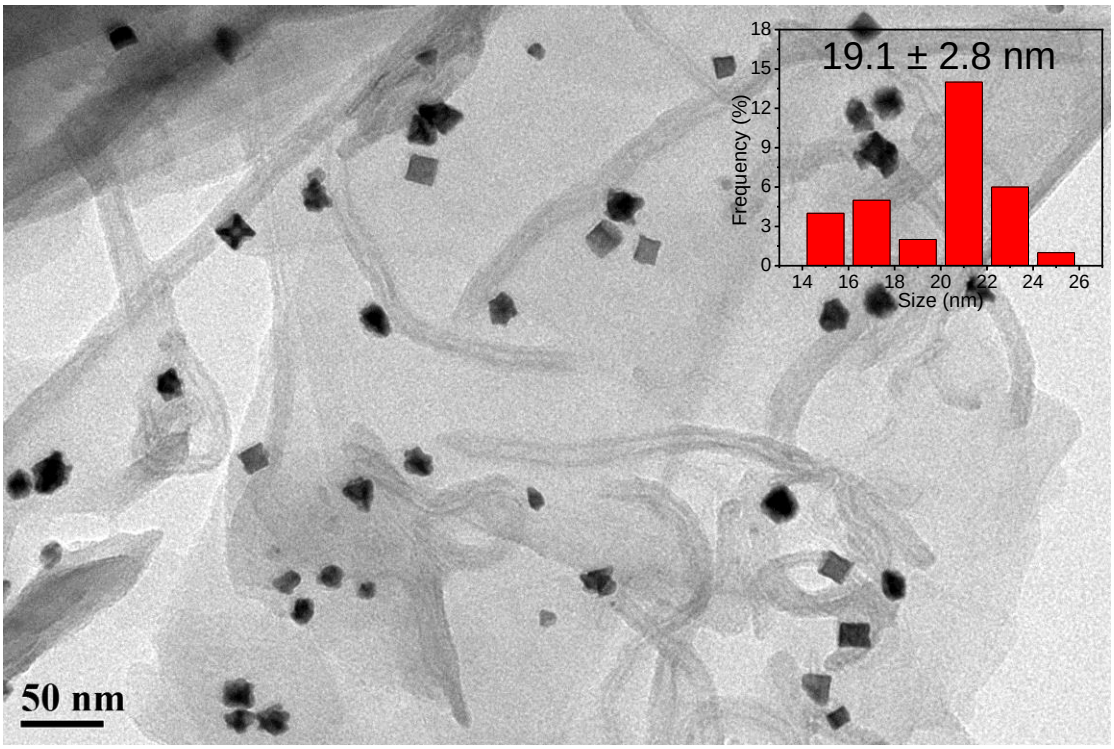

Fig. S11 TEM image (and size-distribution histogram) of PtNi/10G CNCs using common graphene as the support.

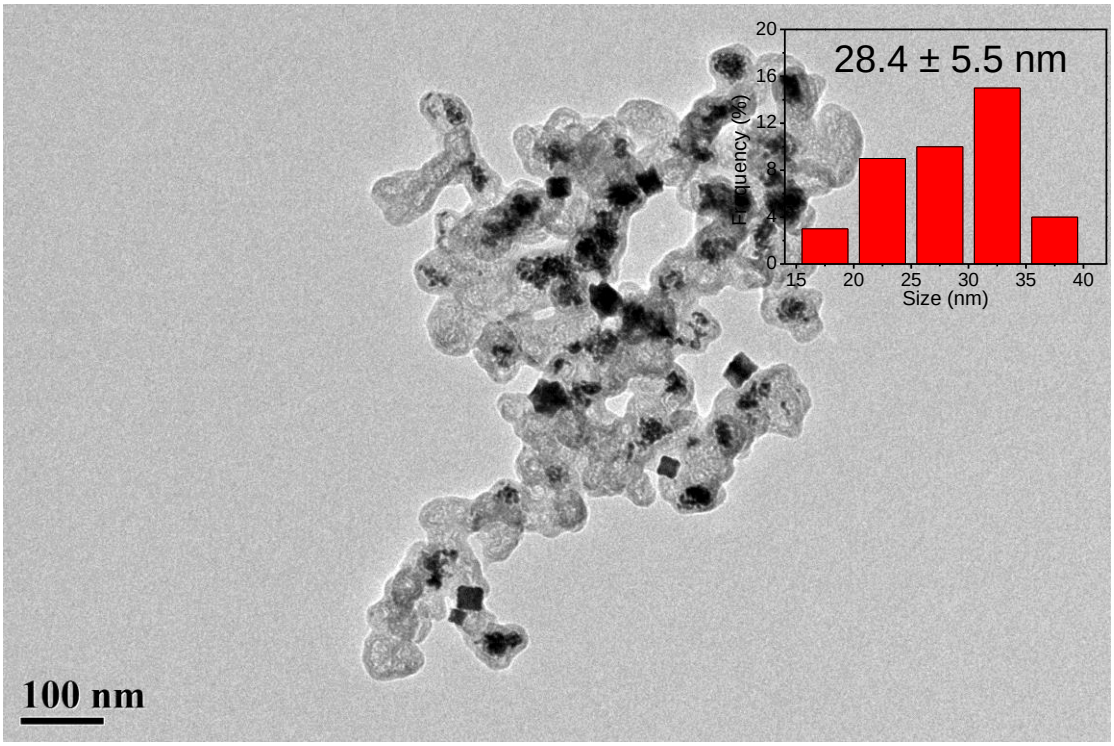

Fig. S12 TEM image (and size-distribution histogram) of PtNi/10C CNCs using Vulcan XC-72 as the support.

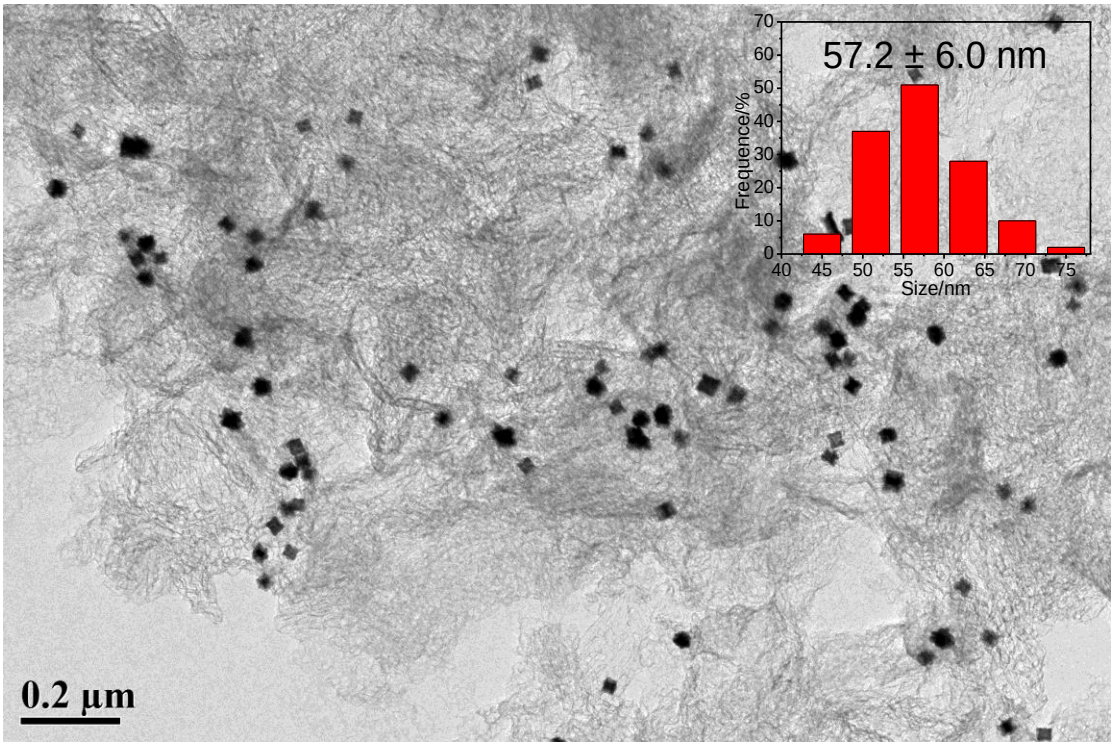

Fig. S13 TEM image (and size-distribution histogram) of PtNi CNCs/10PG using two-step loading method.

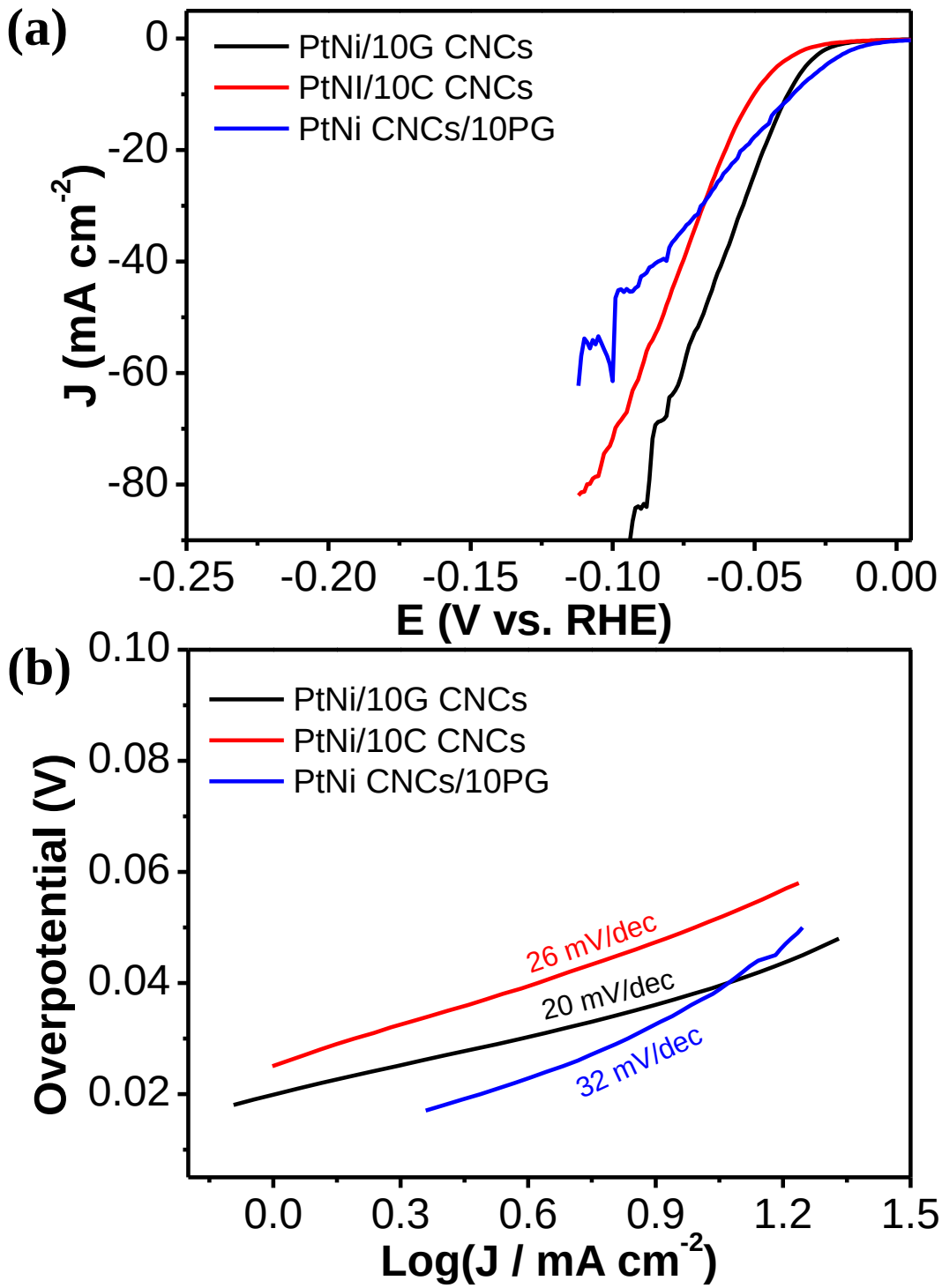

Fig. S14 (a) LSV curves for HER of PtNi/10G CNCs, PtNi/10C CNCs and PtNi CNCs/10PG in N_2-saturated 0.5 M H_2SO_4 with the current density normalized by the ECSA of Pt species; (b) the corresponding Tafel slopes.

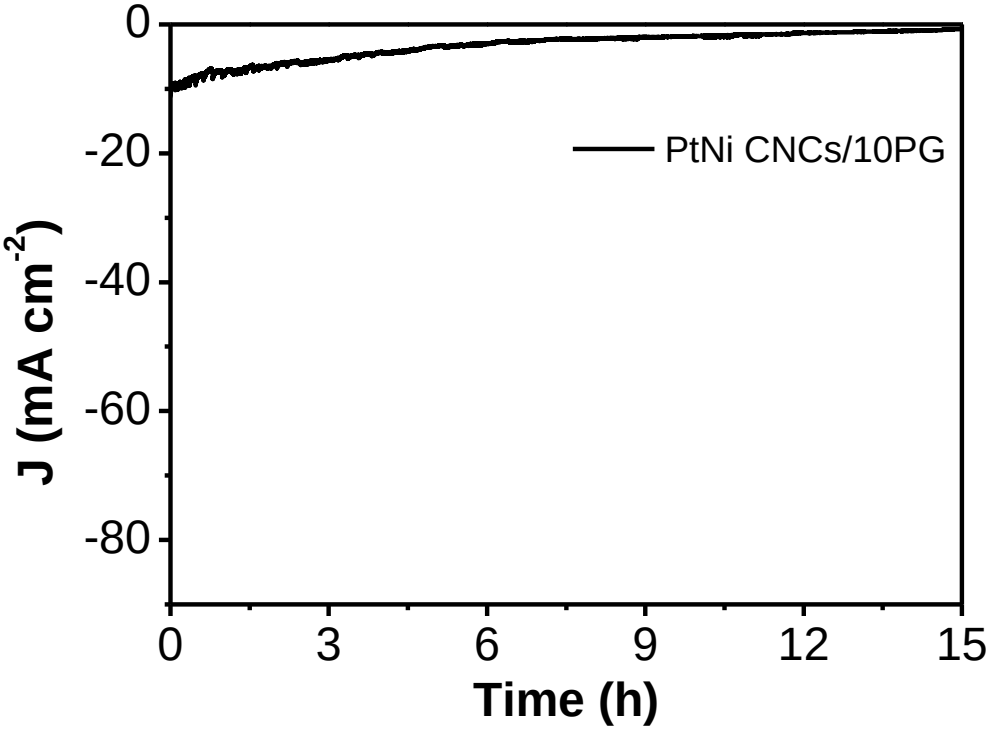

Fig. S15 Chronoamperometric test of PtNi CNCs/10PG for HER with a constant current density of 10 mA cm^{-2} for 15 h.

Table S3 Comparison of catalytic performance of our catalyst and some recently reported representative HER electrocatalytsts in 0.5 M H_2SO_4.

Catalyst	Current density (mA cm^{-2})	Overpotential at corresponding J (mV)	Tafel (mV dec^{-1})	Reference
PtNi/10PG CNCs	10	31	18	This work
Pt NC/N-graphene-2	10	24	28	[4]
Pt-Cu/CNFs-1:2	10	71	68	[5]
Pt NPs/CNFs	10	175	50	[6]
Pt/BCF	10	55	32	[7]
PtAgCo-II	705	400	27	[8]
fct-PtFe	10	7	-	[9]
PtNi@NGNTs	100	143	35	[10]
Pt200-VGNSAs/ CC	10	60	28.5	[11]
PtRu@RFCS-6h	10	19.7	27.2	[12]
Pt-Pd@NPA	10	11.7	31.2	[13]
Pt-Pd-rGO-I	791	300	10	[14]
0.5 wt% Pt-MoO_2/MWCNTs	10	39	43	[15]

Reference

1 G. Ning, Z. Fan, G. Wang, J. Gao, W. Qian and F. Wei, *Chem. Commun.*, 2011, **47**, 5976–5978.

2 M. Crespo-Quesada, J. M. Andanson, A. Yarulin, B. Lim, Y. Xia and L. Kiwi-Minsker, *Langmuir*, 2011, **27**, 7909–7916.

3 K. Y. Cho, Y. S. Yeom, H. Y. Seo, P. Kumar, A. S. Lee, K. Y. Baek and H. G. Yoon, *ACS Appl. Mater. Interfaces*, 2017, **9**, 1524–1535.

4 B. Jiang, F. Liao, Y. Sun, Y. Cheng and M. Shao, *Nanoscale*, 2017, **9**, 10138–10144.

5 J. Wang, J. W. Chen, J. D. Chen, H. Zhu, M. Zhang and M. L. Du, *Adv. Mater. Interfaces*, 2017, **4**, 1–8.

6 T. Yang, M. Du, H. Zhu, M. Zhang and M. Zou, *Electrochim. Acta*, 2015, **167**, 48–54.

7 Y. Mi, L. Wen, Z. Wang, D. Cao, H. Zhao, Y. Zhou, F. Grote and Y. Lei, 2016, **262**, 141–145.

8 A. Mahmood, H. Lin, N. Xie and X. Wang, *Chem. Mater.*, 2017, **29**, 6329–6335.

9 Q. Li, L. Wu, G. Wu, D. Su, H. Lv, S. Zhang, W. Zhu, A. Casimir, H. Zhu, A. Mendoza-Garcia and S. Sun, *Nano Lett.*, 2015, **15**, 2468–2473.

10 X. Bao, J. Wang, X. Lian, H. Jin, S. Wang and Y. Wang, *J. Mater. Chem. A*, 2017, **5**, 16249–16254.

11 H. Zhang, W. Ren, C. Guan and C. Cheng, *J. Mater. Chem. A*, 2017, **5**, 22004–22011.

12 K. Li, Y. Li, Y. Wang, J. Ge, C. Liu and W. Xing, *Energy Environ. Sci.*, 2018, **11**, 1232–1239.

13 C. Yang, H. Lei, W. Z. Zhou, J. R. Zeng, Q. B. Zhang, Y. X. Hua and C. Y. Xu, *J. Mater. Chem. A*, 2018, **6**, 14281–14290.

14 S. Bai, C. Wang, M. Deng, M. Gong, Y. Bai, J. Jiang and Y. Xiong, *Angew. Chemie - Int. Ed.*, 2014, **53**, 12120–12124.

15 X. Xie, Y. Jiang, C. Yuan, N. Jiang, S. Zhao, L. Jia and A. Xu, 2017, 24979–24986.